Scientific Research Publishing

World Journal of Mechanics, 2025, 15(7), 117-133
https://www.scirp.org/journal/wjm
ISSN Online: 2160-0503
ISSN Print: 2160-049X

Distribution of External Load on Multi-Joint Points-New Theoretical Approach

Zouhair Chaib, Christophe Delcher

Assemblies Department, Technical Center for Mechanical Industries (CETIM), Senlis, France
Email: Zouhair.Chaib@Cetim.fr, Christophe.Delcher@cetim.fr

How to cite this paper: Chaib, Z. and Delcher, C. (2025) Distribution of External Load on Multi-Joint Points-New Theoretical Approach. *World Journal of Mechanics*, **15**, 117-133.
https://doi.org/10.4236/wjm.2025.157007

Received: July 1, 2025
Accepted: July 28, 2025
Published: July 31, 2025

Abstract

Today, industrial designers typically rely on two main methods to estimate the external load distribution in bolted assemblies. The first is an analytical model based on the assumption of perfectly rigid bodies, which often fails to accurately identify the critical bolt and its corresponding load. The second method involves Finite Element Analysis (FEA), which is known for its precision but requires significant time, specialized software, and technical expertise. This paper introduces a new analytical approach designed to assist engineers in distributing external loads across connection points, thereby identifying critical connections and their associated loading conditions. The proposed method incorporates key parameters that influence the behavior of each connection point, including its position relative to the applied load, preload, local stiffness, component elasticity, and friction coefficient. The conceptual framework of this approach is presented, along with the derivation of the primary formula used for load distribution calculations. Additional formulas are referenced with appropriate sources. Furthermore, this paper provides FEA simulations and experimental results to validate and discuss the effectiveness of the proposed method. Finally, conclusions are drawn, and future research directions are outlined.

Keywords

External Load Distribution, Bolt Preload, Stiffness, Resilience

1. Introduction

Regarding all the new constraints (environment, energy, material and transportation costs, …), designers work hard to optimize their structure. Given their known advantages, bolted connections are often used in mechanical structures. To optimize these components, designers need a simplified approach (analytical) to pro-

duce a first sketch before performing any FE Analysis or experimental testing. The existing analytical approach (VDI2230 [1], NFE 25030 [2], Cetim-Cobra [3], EN13001 [4], Guillot [5] [6], Alkatan [7], Massol [8], …) provides formulas to calculate the behavior of a single joint (critical fastener). However, most industrial assemblies are defined with multiple connection points. To overcome this limitation, users use some assumptions, e.g., uniform distribution of loads and linear distribution of moments [1] [9]-[15]. For some specific applications, authors [1] [16]-[18] have developed specific analytic approaches to take into account the elasticity of loaded parts: Chakhari [17] used a hybrid approach (Simplified Finite Model) to treat an assembly with two bolts subjected to external axial load. He demonstrates that only the first preloaded bolt supports the full external load before any contact separation of its parts. Paroissien [18] developed a similar model to Chakhari's model: in his model, he treats a hybrid assembly (bonded and riveted) subjected to a shearing load. In those hydride approaches, the adhesive and/or part-contact are considered as spring elements, and the parts are modeled by a series of beam elements, then a global FE matrix is built with appropriate boundary conditions. M. Sinthusiri & Nassar [16] and N. Konkong & K. Phuvoravan [19] have detailed another approach based on springs to represent loaded parts and joints of an assembly subjected to shearing load. Those cited works show very interesting results. On the other side, Geoffrey L. Kulak [20] provides experimental feedback of the load distribution of shared assemblies that confirms the limitation of the basic assumption (uniform and linear distribution of external loads on fastening points). P. Kawecki, A. Kozlowski [21] give a lot of experimental results that confirm previous observations. For slewing bearing, Z. Chaib and A. Daidie [22] and [23] have used in the first time FEA with a specific bearing modeling to calculate the load in each rolling element to study the load distribution on bolts in the second time. They have demonstrated that load distribution depends on a lot of geometric and physical parameters. It demonstrates the utility of using the "Krep" factor in the EN 13001-3-4 standard [2] to amplify loads obtained by the analytic distribution when flange supports of slewing bearings had some stiffeners.

Despite their accuracy, the above-listed models that take into account parts' elasticities are not used in industrial applications for different reasons: the validity of the model is limited to a specific geometry of clamped parts, a specific load, or a specific type of joint (rivet, bolt, adhesive, hybrid…). Another factor that is frequently considered in industrial applications is the ease of use and verification of the approaches used. This criterion is missed by most authors.

The aim of this paper is to identify, using the simplest possible approach, the most critical joint, taking into account the main factors that influence the distribution of external loads.

2. Basic Knowledge about the Preloaded Joints

To ensure a clear understanding of the proposed approach, it is essential to review some fundamental concepts, particularly in the context of preloaded joints. Pre-

loaded joints exhibit complex mechanical behavior influenced by factors such as the level of applied preload, friction coefficients, and external loads acting on each joint. Specifically, in the case of a single-bolt assembly subjected to an axial load (F_a), the resulting load in the bolt (F_b) can be described by a bi-linear relationship, as expressed in Equation (1).

$$F_b = K_b \times \Delta L_b = \max \begin{cases} F_0 + \lambda \times F_a & \rightarrow \textit{Before part separation} \\ F_a & \rightarrow \textit{After part separation} \end{cases} \quad (1)$$

According to Figure 1, the part displacement (separation) at applied load points of each bolt could be defined by Equation (2).

$$\Delta L_{ass} = \Delta L_{b,Fa} + (1-\beta) \times \delta_P \times F_a \quad (2)$$

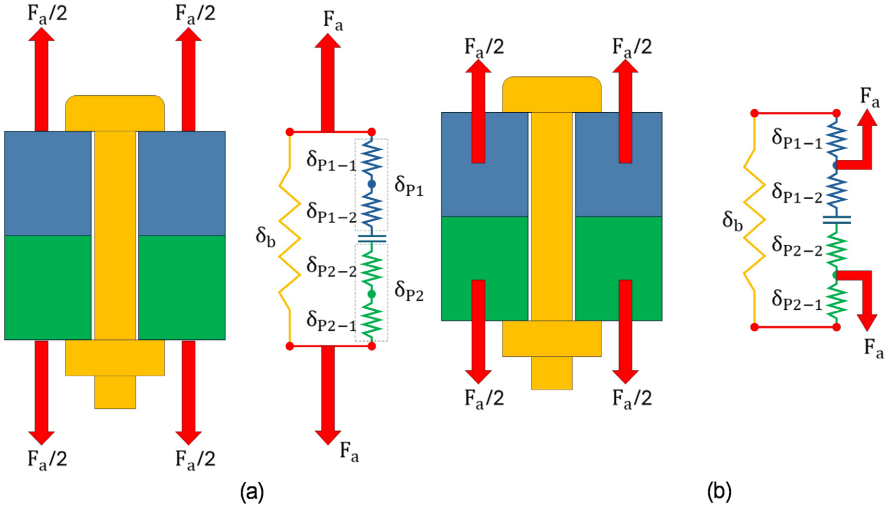

Figure 1. Preloaded assembly with 2 introduction load factors: (a) $\beta = 1$ and (b) $0 < \beta < 1$ (Cetim Cobra [3]).

During assembly loading and before any contact opening, additional bolt elongation is done by: $\Delta L_{b,Fa} = \lambda \times F_a \times \delta_b$. Finally, the local assembly elongation could be expressed by Equation (3).

$$\Delta L_{ass} = \left(\lambda \times \delta_b + (1-\beta) \times \delta_P\right) \times F_a \quad (3)$$

From the last equation, local assembly resilience could be done by Equation (3).

$$\delta_{ass}^{F_a} = \lambda \times \delta_b + (1-\beta) \times \delta_P \quad (4)$$

After contact opening, only the load factor "λ" should be set to 1.

For multi-joints, the displacement at loading point "Δ" is the same for all connections. So, for a joint "i", the total displacement at the loading point is done by the addition of the part-elongation in concerned bolt "i" (due to F_a), and its deflection due to "F_a" and "M_e" as expressed by Equation (5).

Figure 2, Equation (6) and Equation (7) provide an example of a part deflection in case of a prismatic part loaded by an excentric axial load "F_a" and by an external bending moment "M_e". Other formulas could be used for other geometries.

$$\Delta = \Delta L_{P,i} = \Delta L_{ass,i} + \Delta LB_{Pi,Fa} + \Delta LB_{Pi,Me} \tag{5}$$

$$\Delta LB_{Pi,Fa} = \frac{L_i^3}{3 \times E_{Pi} \times I_{Pi}} \times F_a = \frac{L_i^3}{3 \times E_{Pi} \times \frac{w \times h^3}{12}} \times F_a = \delta_{B,Pi}^{Fa} \times F_a \tag{6}$$

$$\Delta LB_{Pi,Me} = \frac{L_i^2}{2 \times E_{Pi} \times I_{Pi}} \times M_e = \frac{L_i^2}{2 \times E_{Pi} \times \frac{w \times h^3}{12}} \times M_e = \delta_{B,Pi}^{Me} \times M_e \tag{7}$$

where:

- L: distance between joint and loading point.
- E_p: Young modulus of loaded part.
- I: Quadratic moment of loaded part, "b" → Part-Width and "h"→ Part Thickness.
- "F_a" and "M_e" are respectively external axial load and external bending moment.
- "Δ" and "θ" are respectively, axial displacement and rotation due to "F_a" and "M_e".

To simplify formulas, the part elongation could be defined by Equation (8).

$$\Delta = \Delta L_{Pi} = \left(\delta_{ass,i}^{Fa} + \delta_{B,Pi}^{Fa}\right) \times F_a + \delta_{B,Pi}^{Me} \times M_e \tag{8}$$

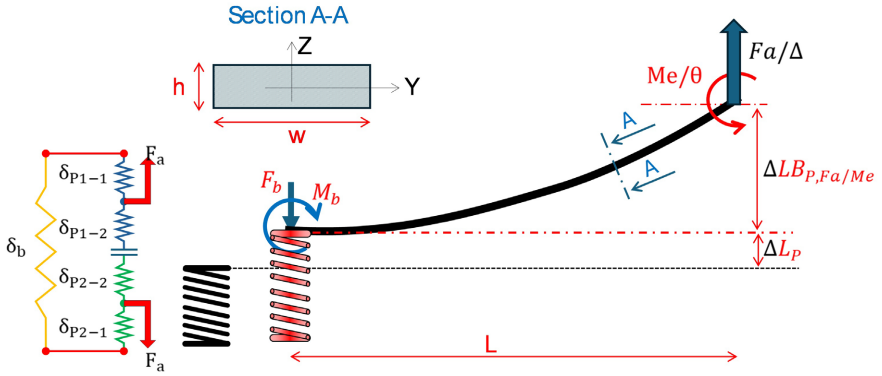

Figure 2. One part elongation under axial external load and bending moment.

The same analysis could be done for any shearing load and sliding moment as shown by **Figure 3** and **Figure 4**. Some specific features should be considered for local behaviors of preloaded joints under any transversal load and bending moment. Indeed, due to preload and friction/adherence coefficient between the clamped parts and at the fasteners bearing surfaces, the assembly could have a complex behavior as illustrated by **Figure 5**. Here, the total displacement/rotation at the loading point is the sum of the local joint movements and the loaded parts elongations. The parts elongations in the "X" and "Y" directions are done by Equation (9) and Equation (10). And the joint movements could be defined by Equation (11).

$$\Delta L_{P,X} = \Delta L_{b,X} + \Delta L_{P,F_{s,x}^{ext}} + \theta_b \times Y_{F_{s,x}^{ext}} \tag{9}$$

$$\Delta L_{P,Y} = \Delta L_{b,Y} + \Delta L_{P,F_{s,y}^{ext}} - \theta_b \times X_{F_{s,y}^{ext}} \tag{10}$$

Before any sliding, bolt deflections ($\Delta L_{P,X}$ & $\Delta L_{P,Y}$) and joint rotation (θ_b) are ignored. Then after sliding those quantities could be calculated using basic notion of material strength. And for most industrial assembly with multi-joints points, the joint rotation is close to zero (0).

$$\Delta L_{P,F_{s,x}^{ext}} = \left(\frac{\left| X_{F_{s,x}^{ext}} \right|}{E_{P1} \times w_{P1} \times b_{P1}} + \frac{\left| X_{-F_{s,x}^{ext}} \right|}{E_{P2} \times w_{P2} \times b_{P2}} \right) \times F_{s,x}^{ext} \tag{11}$$

$$\Delta L_{P,F_{s,y}^{ext}} = \left(\frac{\left| Y_{F_{s,y}^{ext}} \right|}{E_{P1} \times w_{P1} \times L_{P1}} + \frac{\left| Y_{-F_{s,y}^{ext}} \right|}{E_{P2} \times w_{P2} \times L_{P2}} \right) \times F_{s,y}^{ext} \tag{12}$$

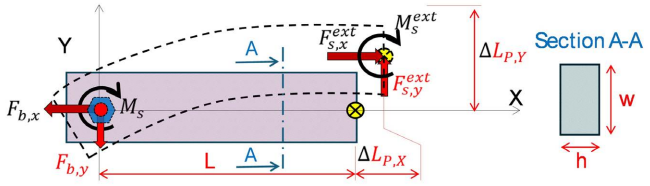

Figure 3. One Part elongation under external shearing load and sliding moment.

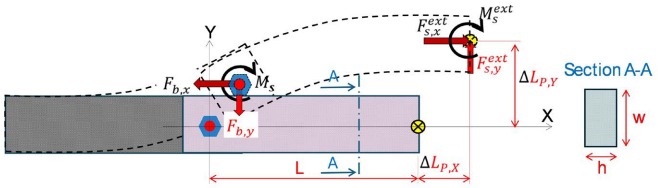

Figure 4. Total elongation of assembly under external shearing load and sliding moment.

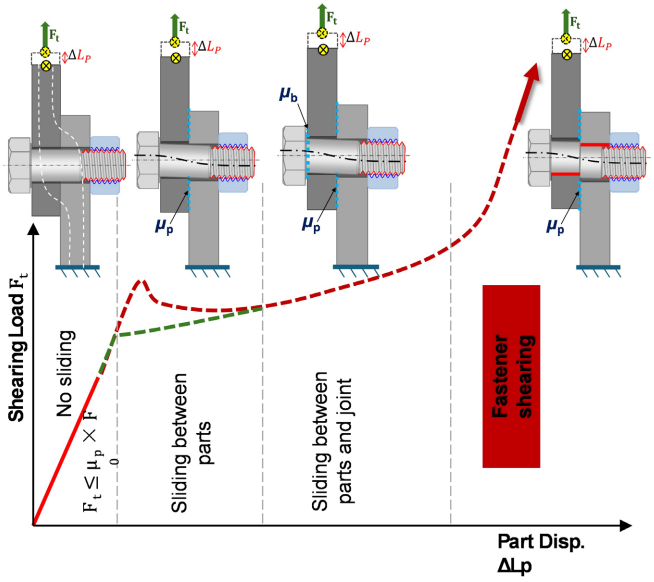

Figure 5. Part elongation under external shearing load.

To ensure a good behaviors of preloaded connections (specially bolted connections), three main practical rules should be taken into account: no sliding between parts (micro or macro), no separation or significant opening at contact surfaces and anticipate or compensate any preload loosening [1]-[8].

3. New Approach to Distribute External Load on Fastening Points

The proposed approach involves distributing external loads across connection points, based on a set of key assumptions:

1- The friction coefficient between parts to be considered is the minimum level of friction coefficient of contacts located between the loaded parts.

2- Loaded parts are modeled by one fixed part at its loading point and by a loaded part as defined by user.

3- For one imposed displacement of the loading point, the load in each joint is independent of the other joints, their number and positions. This assumption considers all individual joints as parallel springs. It is indirectly demonstrated by Chakhari [16] in his study of assembly defined by 2 preloaded joints. In his paper, all results obtained by his developed model, FEA and experimentation demonstrate that the second bolt is not loaded. That means, in any mechanical structure, only the first range of bolts around the loading points is mainly loaded. And the next ranges are loaded only after contact opening or any sliding between loaded parts. **Figure 6** illustrates this assumption: in this figure, colored (red) Hex-Heads represents main loaded joints under applied "Fext" load. Before any contact opening or sliding, other bolts could be ignored.

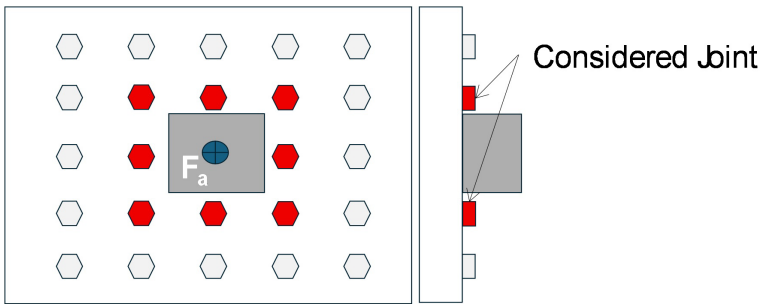

Figure 6. Illustration of considered joints located around applied load.

By considering basic knowledge listed below, two main cases could happen during the application of external load:

Case 1 (Safe Industrial Design): all connection points are conformed to practical rules mentioned above (no sliding, no opening and no separation). In this case, preloaded joints have a linear behavior under any axial and/or any transversal loads. By consequence, internal joint loads could be defined as a function of loading point displacements (Equation (13)).

$$\begin{bmatrix} & & & & & \\ & & & & & \\ & & & & & \\ & & & & & \\ & & & & & \\ & & & & & \end{bmatrix} \times \begin{bmatrix} \Delta L_{P,x} \\ \Delta L_{P,y} \\ \Delta L_{P,z} \\ \Delta\theta_{P,x} \\ \Delta\theta_{P,y} \\ \Delta\theta_{P,z} \end{bmatrix} = \begin{bmatrix} F_{b,x} \\ F_{b,y} \\ F_{b,z} \\ M_{b,x} \\ M_{b,y} \\ M_{b,z} \end{bmatrix} \tag{13}$$

By writing the equilibrium principle for assembly at the loading point, all internal loads could be calculated as function of external loads.

$$\sum \begin{Bmatrix} F_{b,x} & M_{b,x} \\ F_{b,y} & M_{b,y} \\ F_{b,z} & M_{b,z} \end{Bmatrix}_{(x_{Fe},y_{Fe},z_{Fe})} = \begin{Bmatrix} F_{e,x} & M_{e,x} \\ F_{e,y} & M_{e,y} \\ F_{e,z} & M_{e,z} \end{Bmatrix}_{(x_{Fe},y_{Fe},z_{Fe})} \tag{14}$$

$$\sum_{i=1}^{n} \begin{bmatrix} & & & & & \\ & & & & & \\ & & & & & \\ & & & & & \\ & & & & & \\ & & & & & \end{bmatrix} \times \begin{bmatrix} \Delta L_{P,x} \\ \Delta L_{P,y} \\ \Delta L_{P,z} \\ \Delta\theta_{P,x} \\ \Delta\theta_{P,y} \\ \Delta\theta_{P,z} \end{bmatrix} = \begin{bmatrix} F_{e,x} \\ F_{e,y} \\ F_{e,z} \\ M_{e,x} \\ M_{e,y} \\ M_{e,z} \end{bmatrix} \tag{15}$$

This approach could be divided into many simplified approaches: distribution of axial load, transversal load, bending moment and sliding moment.

For axial load ($F_a \neq 0$, $M_e = 0$), by using Equation (14) and Equation (8), the axial displacement could be calculated by using Equation (16). And the axial load supported by each joint "*i*" could be estimated by Equation (17).

$$\Delta = \frac{F_a}{\sum_{i=1..n} K_{eq}^{ass,i}} \tag{16}$$

$$F_a^{joint,i} = \frac{K_{eq}^{ass,i}}{\sum_{i=1..n} K_{eq}^{ass,i}} F_a \tag{17}$$

where $K_{eq}^{ass,i} = \frac{1}{\delta_{ass,i}^{Fa} + \delta_{B,Pi}^{Fa}}$ is the equivalent stiffness between the joint "*i*" and the loading point.

Case 2 (Unsafe Industrial Design): The is a risk of sliding or joint opening. In this case the load distribution cannot be linear when external load is applied, and other phenomena may occur (settlement, spontaneous unscrewing, …) that leads to loosening preload after unloading the structure. Here, only iterative calculations could be applied, and in each iteration, stiffness will be updated regarding residual load or residual displacement at each joint.

3.1. Distribution of Axial Load—Case of Rectangular Plate Assembled to a Stiff Support with 4 Bolts Located around Loading Point

To illustrate this approach, a simplified assembly of rectangular plates with 4 bolts M10-10.9 has been selected. Assembly data is provided by Table 1 and Figure 7.

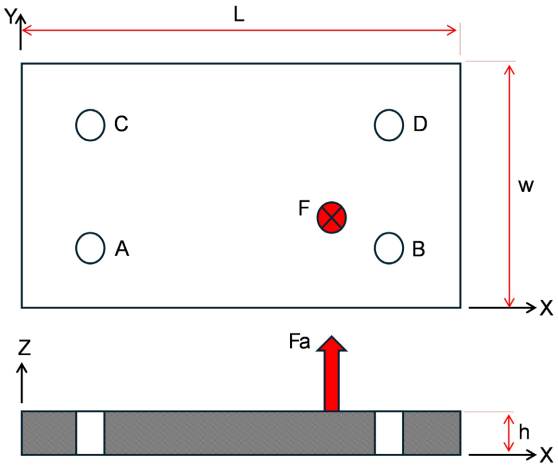

Figure 7. Assembly #1, case of rectangular plate subjected to an axial load.

Table 1. Geometrical data of Assembly #1.

	X [mm]	Y [mm]	Z [mm]	F_0 [N]	$F_{a,\ separation}$ [N]
Plate (L x W x h)	100	100	10		
A	25	25	10	25,000	26,929
B	75	25	10	20,000	21,543
C	25	75	10	15,000	16,157
D	75	75	10	10,000	10,772
F, assembly #1	50	50	10	25,000	26 929
F, assembly #2	60	25	10		

Table 2. Geometrical and calculated data of Assembly #1.

Total Applied Load [N]				43,092				60,757	
Step Load [N]			Step 1	43,092		Step 2	17,665		
Part-Thickness 10 mm			Good Preloading			Preload Effect			
Li [mm]	W i [mm]	IGZ [mm^4]	$K_{ass,i}$ [N/mm]	$F_{a,i\ step}$ [N]	$F_{a,i}$ [N]	$K_{ass,i}$ [N/mm]	$F_{a,i\ step}$ [N]	$F_{a,i}$ [N]	
35.36	141.42	94,281	767,504	10,773	10,773	767,504	5385	16,158	
35.36	141.42	94,281	767,504	10,773	10,773	767,504	5385	**16,158**	
35.36	141.42	94,281	767,504	10,773	10,773	767,504	5385	16,158	
35.36	141.42	94,281	767,504	**10,773**	10,773	215,283	1510	12,283	
Total joints stiffness [N/mm]				3,070,016		2,517,795			

74,557			84,471			90,000		
Step 3	13,800		Step 4	9914		Step 5	5529	
Preload Effect			Preload Effect			Preload Effect		
$K_{ass,i}$ [N/mm]	$F_{a,i\ step}$ [N]	$F_{a,i}$ [N]	$K_{ass,i}$ [N/mm]	$F_{a,i\ step}$ [N]	$F_{a,i}$ [N]	$K_{ass,i}$ [N/mm]	$F_{a,i\ step}$ [N]	$F_{a,i}$ [N]
767,504	5389	21,547	767,504	5383	**26,930**	215,283	1382	28,312
767,504	5389	**21,547**	215,283	1510	23,057	215,283	1382	24,439
215,283	1511	17,669	215,283	1510	19,180	215,283	1382	20,562
215,283	1511	13,795	215,283	1510	15,305	215,283	1382	16,687
1,965,574			1,413,353			861,132		

For each joint, an equivalent rectangular beam could be calculated. This beam is defined by its length (distance from point "F"), its width, and its quadratic moment as indicated in Table 2. By ignoring the effect of the bending moment in Equation (3), the distribution of external load obtained by applying this approach is detailed in Table 2. This table shows 4 steps to calculate the axial load supported by individual joint. Each step represents a portion of the external load until the beginning of any contact separation in active joint-contact (bold and underlined data). For the first case (Assembly #1), 5 steps are used. Then, due to the bi-linear behaviors of joint, the stiffness of each joint, having a contact opening, was updated (the ratio of stiffness before and after contact opening is close to 10).

Graphs of Figure 8 show the load-distribution on bolts for two cases where the position of applied load is modified. It demonstrates the sensitivity of proposed model to assembly factors, bolt preloads, and to load levels and its positions.

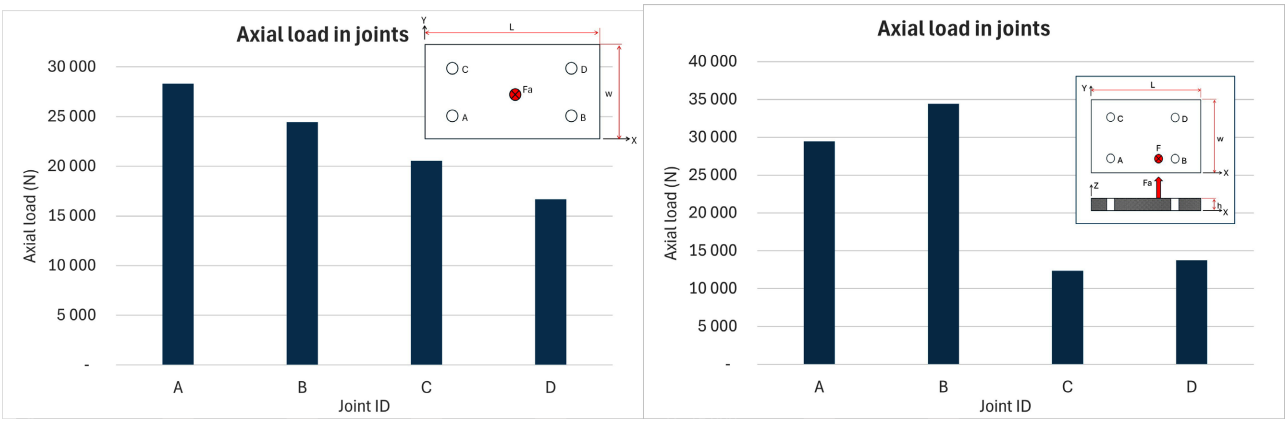

Figure 8. Load distribution, 90 kN applied to assembly#1 at two different positions.

3.2. Distribution of Axial Load—Case of Rectangular Plate Assembled to a Stiff Support with 2 Bolts Located in Series with Loading Point

To evaluate the relative errors introduced by assumption 3 above, Chackari assembly is used as reference. This assembly could be treated as shown by Figure 9. Mentioned resiliencies are done by Equations (4) and (6).

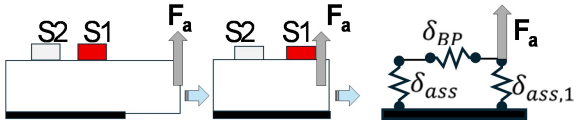

Figure 9. Load distribution, case of beam with 2 bolts subjected to external force "F_a".

Finally, the axial load distributed over each individual assembly (S1 & S2) is given by Equations (18) and (19). Those equations demonstrate the consistency of the 3rd assumption. They demonstrate that the load supported by the second bolt (S2) depends highly on the resilience of the first one and the bending resilience of the loaded part.

$$F_{a,1} = \frac{\delta_{ass,2} + \delta_{BP}}{\delta_{ass,1} + \delta_{ass,2} + \delta_{aBP}} Fa \tag{18}$$

$$F_{a,2} = \frac{\delta_{ass,1}}{\delta_{ass,1} + \delta_{ass,2} + \delta_{aBP}} Fa \tag{19}$$

Using CHAKHARI assembly (L_p = 25 mm, w = 40 mm, th = 20 mm and E_p = 74000 MPa and load introduction factor β = 0.5) and using the half of the bolt and part resiliencies, because only the loaded part is considered ($\delta_b = 3.3410^{-6}$ mm/N and $\delta_p = 4.2110^{-7}$ mm/N), the external load carried respectively by the first and the second bolts before any contact opening are: 26.5 kN (88% F_a) and 3.4 kN (12% F_a).

3.3. Experimental and Numerical Validations of New Formulas

To validate this work, some experimental tests and numerical analysis (FEA) have been done. In this paper, we present the results of two cases. The first one involves a welded structure bolted to a "stiff" support with 10 bolts H M10x60-10.9. This support is locked to the tensile machine frame, then a compressive and a tensile load is applied as shown in Figure 10 and Figure 12. And the second case involves a simple plate bolted to the same support and loaded at four (4) points as shown by Figure 11 and Figure 13. The axial load and the bending moment in the bolts are measured by using three (3) extensiometric gauges installed on a reduced section of the screw and positioned at 0˚, 90˚ and 180˚.

As performed by Figure 11, the external load is applied to assembly #2 by a threaded rod. For both assemblies, the stiff support was fixed by four (4) screws (not visible) and five additional locking supports. Due to these locking conditions, we have considered in the FEA model (Figure 12 and Figure 13) a full locking of this stiff support.

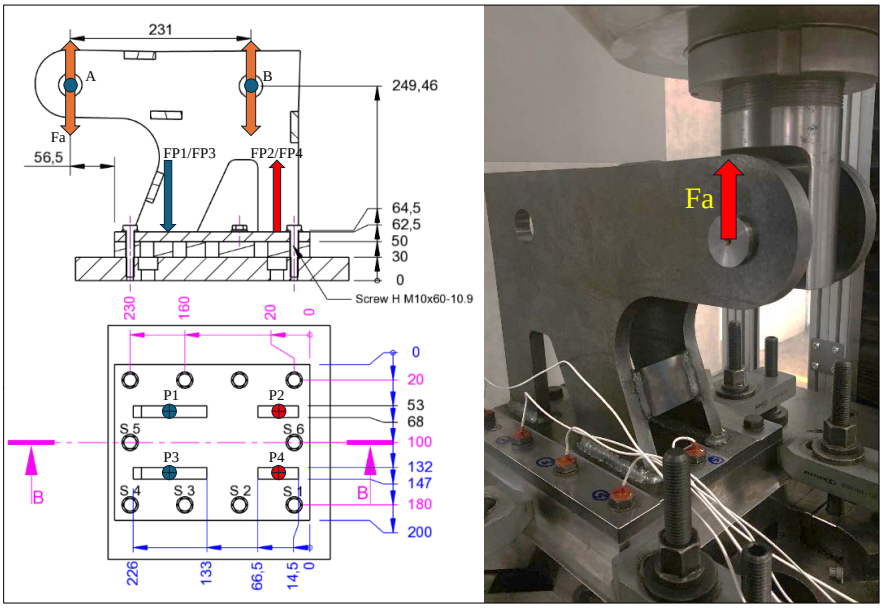

Figure 10. Test-bench #1 bolted to a stiff support and loaded by an external force "F_a".

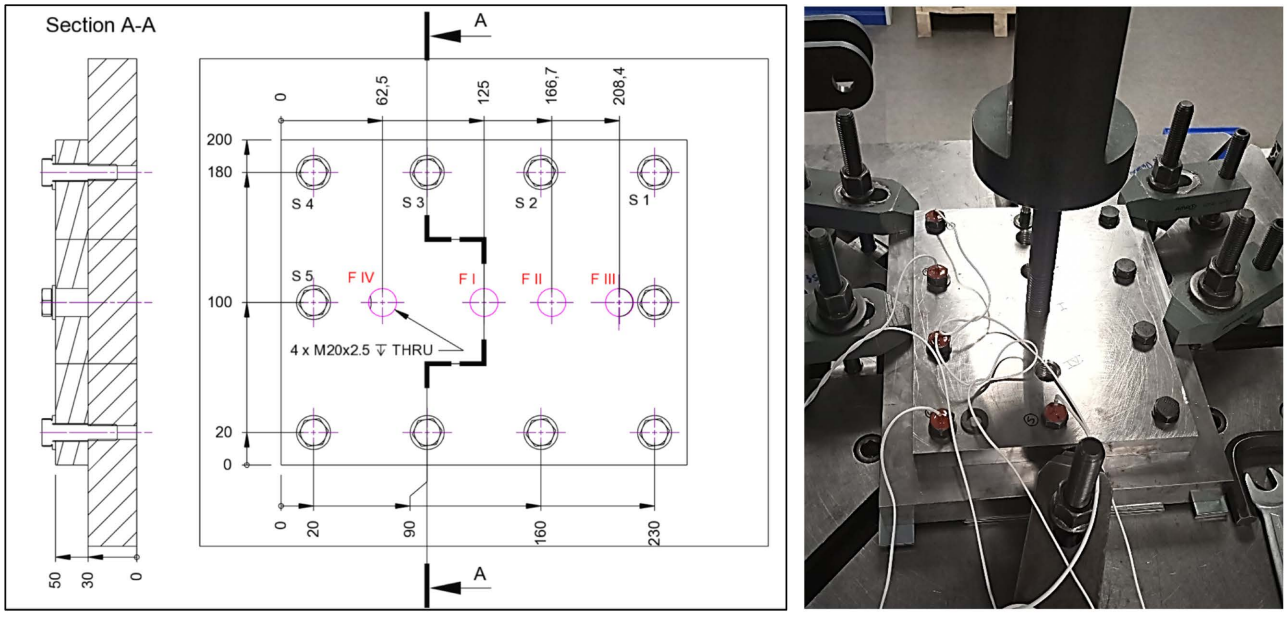

Figure 11. Test-bench #1 (Flat plate).

To apply the developed approach on the first test-bench, the welded shapes (vertical shapes) had been replaced by 4 loading points (FP_1 to FP_4) as used by S. Oman [24]. Although this hypothesis is not relevant (**Figure 12**), it is widely used by industrial designers due to its simplicity: it supposes a unform stress distribution at each welded junction.

By using the symmetry of the shape and the applied load, we consider the equality of the loads ($FP_1 = FP_3$) and ($FP_2 = FP_4$). Finaly, using the static equilibrium principle, FP_1, FP_2, FP_3 and FP_4 could be calculated by Equations (20) and (21) when "F_a" is applied at the point "A".

$$FP_1 = FP_3 = \frac{\overrightarrow{AP_2}}{\overrightarrow{P_1P_2}} \times \frac{F_a}{2} \tag{20}$$

$$FP_2 = FP_4 = \left(1 - \frac{\overrightarrow{AP_2}}{\overrightarrow{P_1P_2}}\right) \times \frac{F_a}{2} \tag{21}$$

Secondly, in order to simplify calculations using VDI 2230 and the developed approach on the second test bench, the M20 holes used to apply the external load are not considered.

To validate the analytical approaches by using FEA and experimental results, we encountered a problem:

1- By using FEA and experimental measurements, only the additional load/moment seen by each bolt could be measured: there is no way to calculate the external load supported by each individual assembly. This fact is due to the load factor "λ" introduced by the bolt preload.

2- By using analytical approaches, external loads supported by each joint are calculated. To convert those quantities into additional loads/moment, accurate

load factors are required. Because this factor depends on a lot of factors as mentioned in most the references listed, analytical formulas are limited to some part-forms and assumptions [1]-[6].

Note: the proposed approach needs a basic load factor for a concentric load and revolution assembly (an estimated value of 10% to 20% could be used for industrial assemblies).

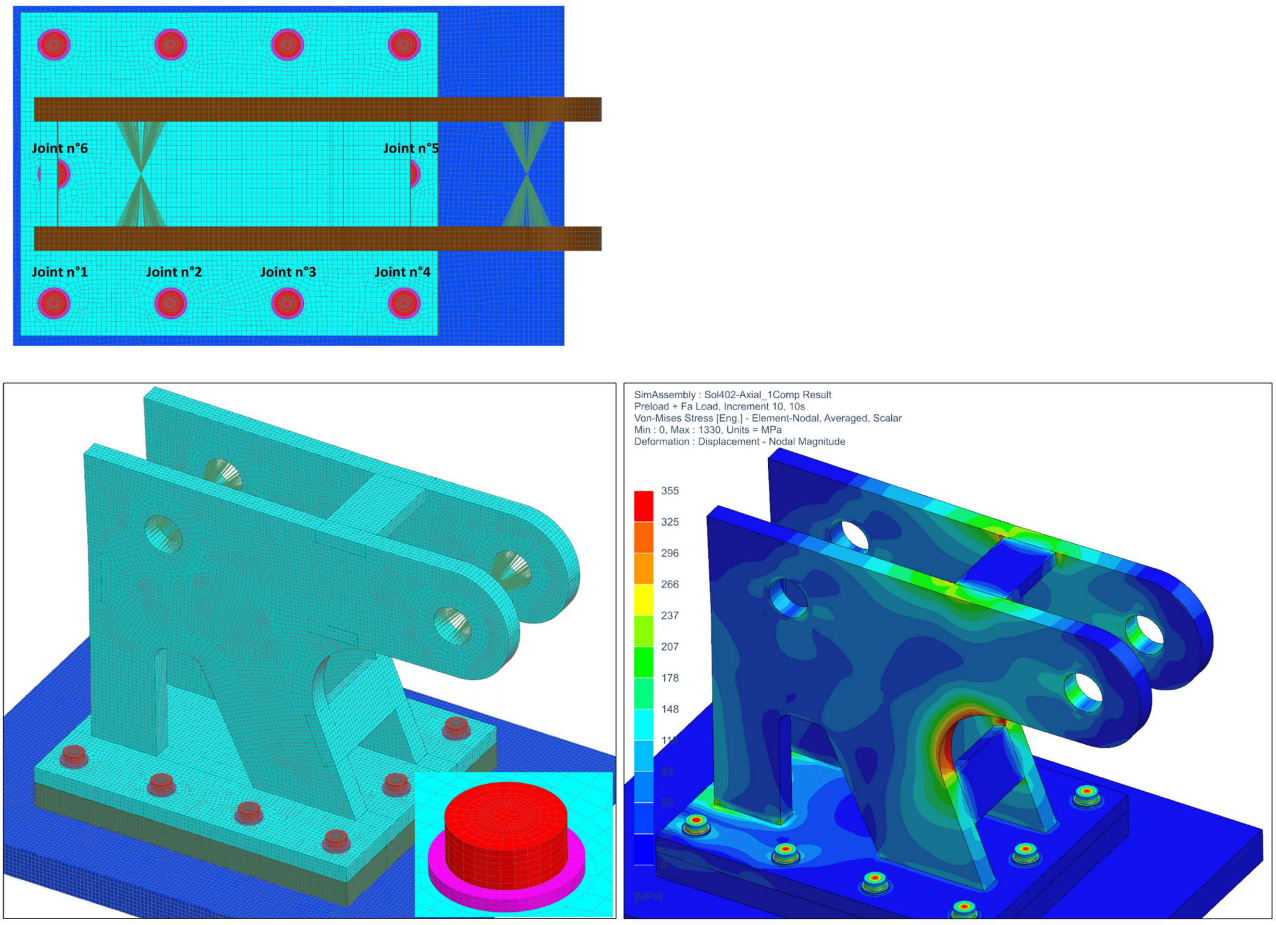

Figure 12. FEA model of Test-bench #2.

Regarding this problem and the inaccuracy of analytical calculations of load-factor, graphs of two vertical axes have been used to validate analytical approaches. The first shows the additional load on the bolt concerned (available for FEA and experimental results) and the second shows the external load on the joint concerned, calculated using the new approach and the VDI 2230-2.

The total external load applied to the full assembly used to build graphs below is 70 kN. For this load, and in case of welded structure (**Figure 10**) FP_1 and FP_2 (equations (20) and (21)) are estimated respectively to:

- Case 1: "F_a" is applied at point "A": 64.37 kN and −29.37 kN
- Case 2: "F_a" is applied at point "B": 8.44 kN and 26.5637 kN

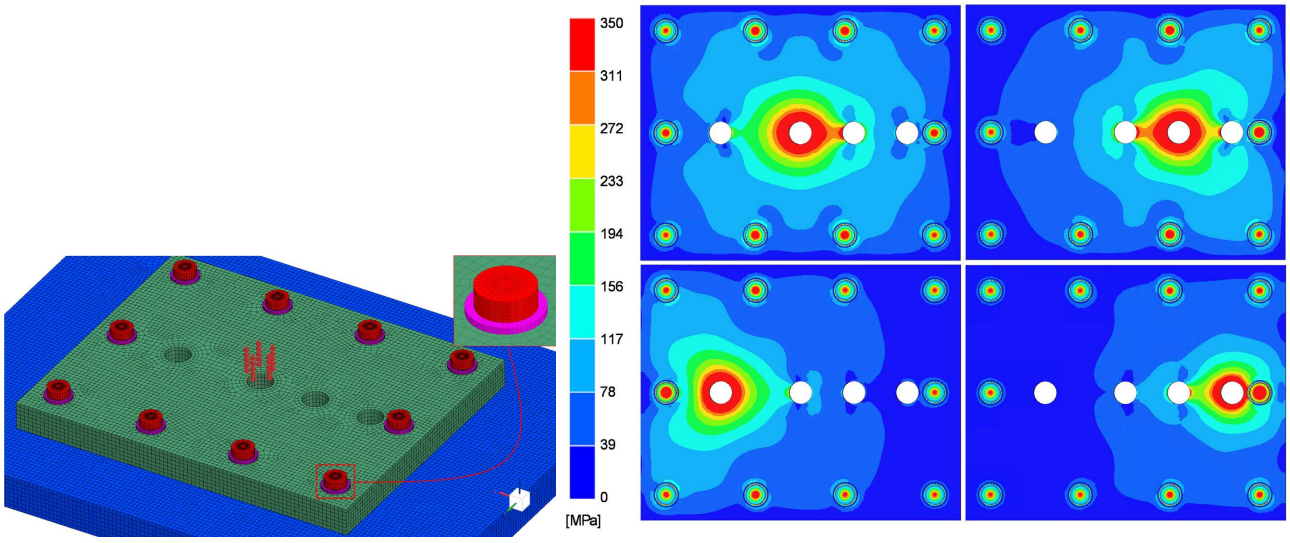

Figure 13. FEA model of Test-bench #2.

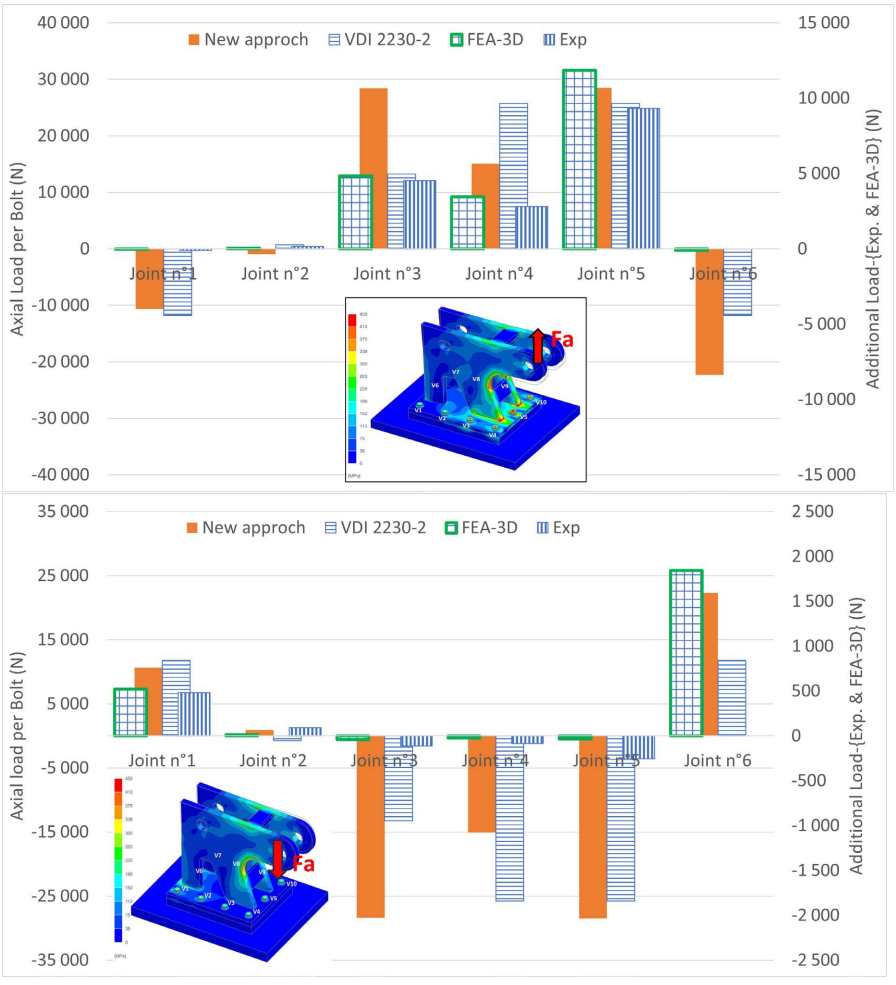

Figure 14. Additional load and calculated loads – External loads at the point "A".

Results given by new approach are obtained by iterative calculations that update

the assemblies resilience after each contact opening.

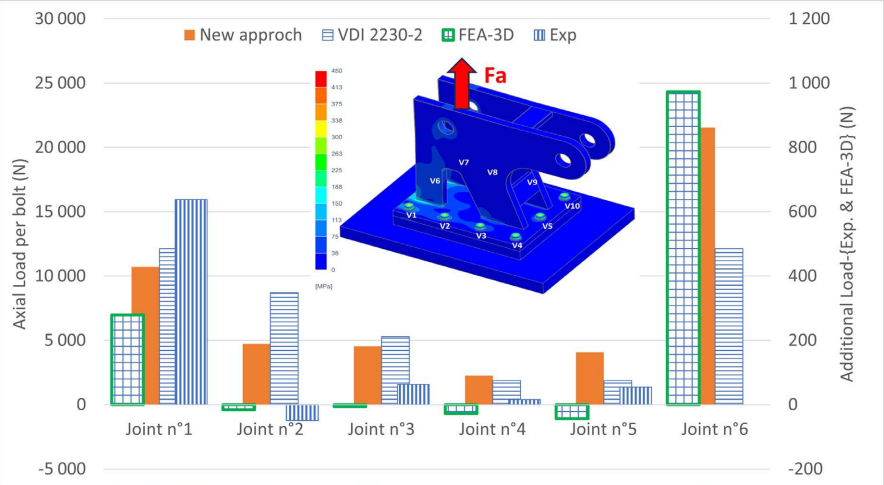

Figure 15. Additional load and calculated loads—external load at the point "B".

Results illustrated in Figure 14 and Figure 15 show a difference in results between the proposed approach and the VDI 2230 approach. Also, they show some difference between the additional load obtained by FEA and by tests when an external load is applied at point "B".

By comparing the measured additional load, which is representative of the external load supported by the joints and with the calculated loads, we can note that the proposed approach accurately identifies the critical joints (higher load level).

Graphs of Figure 16 and Figure 17 show a good correlation between FEA results and those calculated by the proposed approach. When an external load is applied at the point "II", there is a certain difference between the load distribution calculated by proposed approach and FEA. This difference is due to the hole M20 provided for loading the plate at the point "III", which was not taken in account when applying the proposed approach.

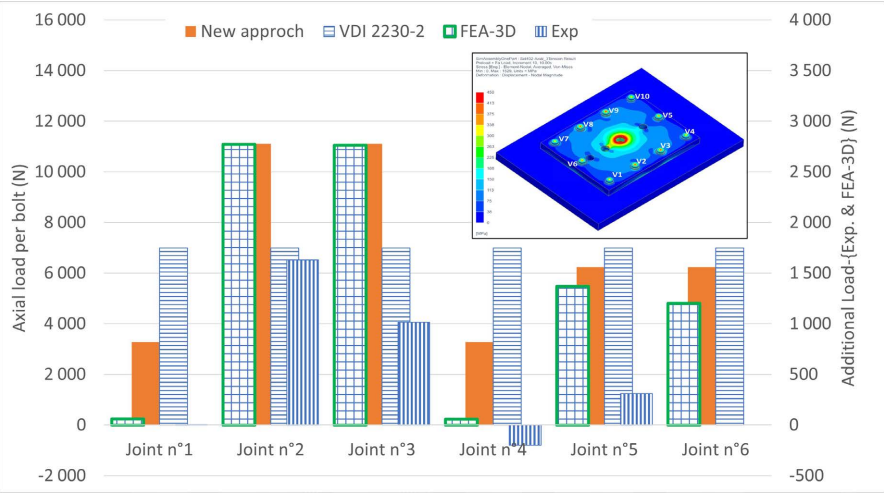

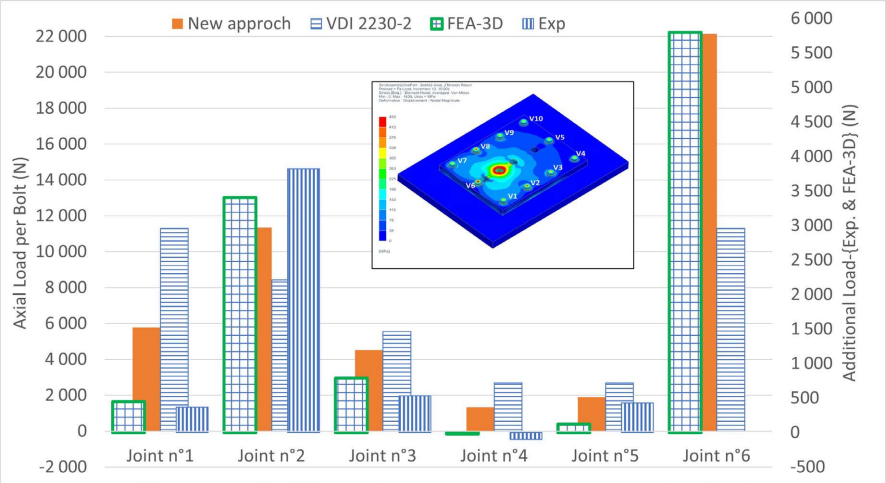

Figure 16. Additional load and calculated loads – External load at the point "I" and "II".

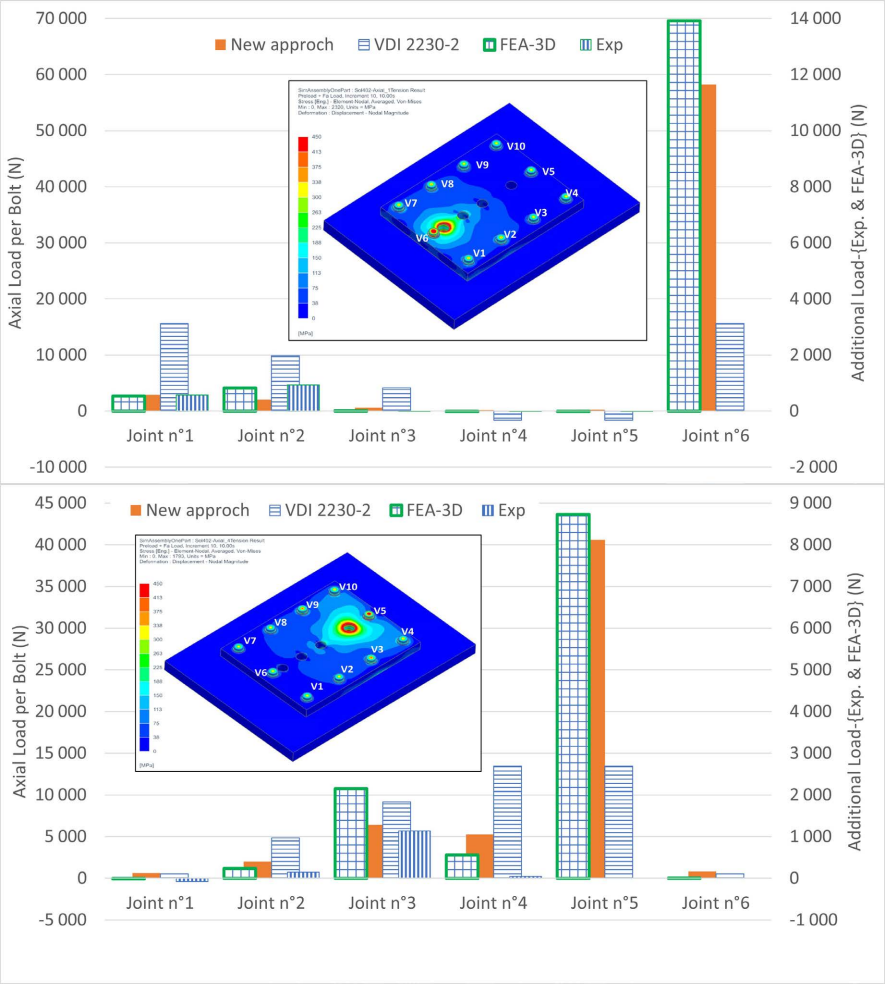

Figure 17. Additional load and calculated loads – External load at the point "III" & "IV".

By considering a same load factor of 20% for 4th loading cases (Point I to Point IV), the relative errors between FEA and proposed approach, at the most loaded

joint are respectively: 1%, −5%, 5% and 16%.

4. Conclusions

This paper introduces a new analytical method designed to assist engineers in distributing external loads on preloaded bolted assemblies. The proposed approach takes into account key factors that influence load distribution, including geometric parameters (such as thickness, width, spacers, joint positions, and diameters), material properties of the loaded components (Young's modulus), and the bolt preload applied to each joint. It's mainly available for assemblies designed to prevent contact opening and sliding between loaded parts. An iterative approach could extend its validity area.

In order to validate the analytical formulas, experimental tests and finite element analysis (FEA) were performed on two representative industrial assemblies: a simple flat plate and welded plates. The results obtained from the analytical method were indirectly compared with those from FEA and experimental studies. These comparisons demonstrate a strong correlation, confirming that the method accurately identifies the most stressed joints.

In a future paper, a complementary study will present the application of this approach to assemblies subjected to shear loads.

Conflicts of Interest

The authors declare no conflicts of interest regarding the publication of this paper.

References

[1] VDI 2230 (2014) Systematische Berechung Hochbeanspruchter Schraubenverbindungen Zylindrische Einschraubenverbin-dungen.

[2] NF E 25030 (2014) Fixations—Assemblages vissés à filetage métrique ISO—Partie 2: Règles de conception pour les assemblages précontraints—Démarche complete.

[3] Theorical Handbook of CETIM-COBRA Software. https://www.cetim.fr/logiciels/cetim-cobra/

[4] EN 13001-3.4 (2018) Cranes—General Design—Part 3-4: Limit States and Proof of Competence of Machinery—Bearings.

[5] Guillot, J. (1989) Assemblages par éléments filetés, Techniques de l'Ingénieur, traité Génie mécanique-B 5 560.

[6] Guillot, J. (1997) Assemblages par éléments filetés. Modélisation et calcul: Techniques de l'Ingénieur BM 5 563.

[7] Alkatan, F. (2005) Modélisation des raideurs des assemblages par éléments filetés précontraints. Master's Thesis, INSA de Toulouse.

[8] Massol, J. (1998) Étude des assemblages boulonnés à chargement faiblement excentré soumis à des sollicitations de fatigue. Master's Thesis, INSA de Toulouse.

[9] NF EN 1993-1-8 (2005) Eurocode 3—Calcul des structures en acier—Partie 1-8: Calcul des assemblages.

[10] BNCM/CNC2M—N0175 (2015) Recommandation pour le tensionnement des assemblages selon la NF 1993-1-8.

[11] Offshore Standards—DNVGL-OS-C101 (2019) Design of Offshore Steel Structures, General—LRFD Method

[12] Bickford, J.H. (2007) Introduction to the Design and Behavior of Bolted Joints Non-Gasketed Joints. Fourth Edition, CRC Press.

[13] Robert, W. and Messler, J.R. (1993) Joining of advanced Material. Butterworth-Heinemann.

[14] Welch, M. (2018) Classical Analysis of Preloaded Bolted Joint Load Distributions. *International Journal of Structural Integrity*, **9**, 455-464. https://doi.org/10.1108/ijsi-07-2017-0045

[15] Welch, M. (2019) A Paradigm for the Analysis of Preloaded Bolted Joints. *Strojnícky časopis—Journal of Mechanical Engineering*, **69**, 143-152. https://doi.org/10.2478/scjme-2019-0012

[16] Sinthusiri, C. and Nassar, S.A. (2021) Load Distributions in Bolted Single Lap Joints under Non-Central Tensile Shear Loading. *Journal of Advanced Joining Processes*, **3**, Article ID: 100055. https://doi.org/10.1016/j.jajp.2021.100055

[17] Chakhari, J. (2007) Modélisation d'une fixation par éléments filetés d'une structure à forte excentration de chargement et soumise à des sollicitations de fatigue. Master's Thesis, INSA de Toulouse.

[18] Paroissien, E. (2006) Contribution aux assemblages hybrides (boulonnés/collés)—Application aux jonctions aéronautiques. Master's Thesis, Université de Toulouse III.

[19] Konkong, N. and Phuvoravan, K. (2017) An Analytical Method for Determining the Load Distribution of Single-Column Multibolt Connection. *Advances in Civil Engineering*, **2017**, Article ID: 1912724. https://doi.org/10.1155/2017/1912724

[20] Kulak, G.L., Fisher, J.W. and Struik, J.H.A. (1987) Guide to Design Criteria for Bolted and Riveted Joints. 2nd Edition, American Institute of Steel Construction, Inc.

[21] Kawecki, P. and Kozlowski, A. (2020) Experimental Investigation of End-Plate Splices with Multiple Bolt Rows of Large Girders. *Journal of Constructional Steel Research*, **167**, Article ID: 105859. https://doi.org/10.1016/j.jcsr.2019.105859

[22] Chaib, Z. (2008) Étude du comportement des fixations par vis des couronnes de guidage de grand diamètre: Élaboration d'un outil de dimensionnement. Master's Thesis, INSA de Toulouse.

[23] Daidié, A., Chaib, Z. and Ghosn, A. (2008) 3D Simplified Finite Elements Analysis of Load and Contact Angle in a Slewing Ball Bearing. *Journal of Mechanical Design*, **130**, Article ID: 082601. https://doi.org/10.1115/1.2918915

[24] Oman, S. and Nagode, M. (2017) Bolted Connection of an End-Plate Cantilever Beam: The Distribution of Operating Force. *Strojniški vestnik—Journal of Mechanical Engineering*, **63**, 617-627. https://doi.org/10.5545/sv-jme.2017.4638